

# Observation of small sub-pulses generated in the DISC-type all-optical wavelength converter

Jun Sakaguchi<sup>1</sup>, Mads L. Nielsen<sup>2</sup>, Takashi Ohira<sup>1</sup>, Rei Suzuki<sup>1</sup> and Yoshiyasu Ueno<sup>1</sup>

<sup>1</sup>University of Electro-Communications, Dept. of Electronics Engineering, 1-5-1, Chohugaoka, Chohu, Tokyo 182-8585, Japan, Tel: +81-424-43-5207, Fax: +81-424-43-5207, Email: sakaguchi@ultrafast.ee.uec.ac.jp

<sup>2</sup>Research Center COM, Technical University of Denmark

**Abstract:** Previously small sub-pulses generation in DISC was predicted as a potential problem. In this work, its existence and mechanism were experimentally verified.

## 1 Introduction

Several types of SOA-based all-optical gates have intensively been studied, for realizing ultrafast, compact, low-power-consumption signal processors for use in future OTDM-WDM network systems. Particularly, the 168-Gb/s error-free wavelength conversion and the 40-Gb/s error-free ultralong-distance 2R transmission experiments have been demonstrated [1, 2] with using DISC-type wavelength converters [3, 4].

Recent modeling research works [5, 6] of the DISC have, however, revealed a potential issue in its fundamental principle; When we minimize the pattern-induced amplitude noise that is often generated inside the DISC, it potentially generates small 'sub-pulses' instead, between the RZ-formatted output pulses. The modeling works have suggested this issue had existed in the above-mentioned experiments.

In this work, in the processes of modeling the previous demonstration experiments and also clarifying the origin of the large amplitude noise in the 168-Gb/s converted eye in Ref. 1, we experimentally verify the existence of those sub-pulses.

## 2 Experimental setup and the theoretical model

Fig. 1 shows our experimental setup, where a commercially available SOA module (InPhenix IPSAD1503, drive current=250 mA) was used. The MZI contained a calcite crystal (DGD,  $\Delta t=5$  ps). The optical phase bias  $\Delta\Phi_B$  between the fast and slow cw components passing through the MZI was tuned by rotating the quarter-wave plate  $Q_1$  and a polarizer  $P_1$ .

The 25-GHz and 12.5-GHz continuous input pulses ( $\lambda_1=1560$  nm) were generated with a mode-locked fiber-ring laser (Pritel UOC-3) and an optical multiplexer. The width of the pulses to the DISC was broadened from 2.2 ps to 3.8 ps with a

100-meter-long single-mode fiber to suppress carrier-heating-related phenomena inside the SOA. The polarization directions of the cw light ( $\lambda_2=1548$  nm, +8.9 dBm) from a DFB LD and the pulses to the SOA input facet were aligned to either TE or TM axis of the SOA. For observing the wavelength-converted output waveforms from the DISC with a very short time resolution, we used a cross-correlator (Femtochrome) to which the 2.2-ps, 12.5-GHz pulses were injected as probe pulses.

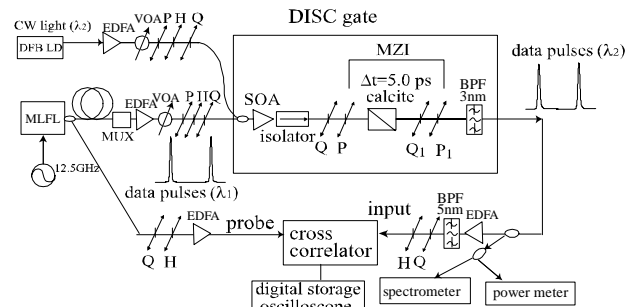


Figure 1. Setup of the DISC-gate experiment.  
VOA: variable optical attenuator, MZI: Mach-Zehnder Interferometer, SOA: semiconductor optical amplifier, Q: quarter-wave plate, H: half-wave plate, P: polarizer,

The mechanism of DISC operation has been modeled based on a rate equation of the carrier density in the SOA as,

$$\frac{d}{dt} \overline{n_c(t)} = \frac{I_{op}}{qV} - \frac{\overline{n_c(t)}}{\tau_c} - \frac{1}{V} \cdot \{G[\overline{n_c(t)}] - 1\} \cdot \frac{|E_{cw}|^2 + |E_{pulse}(t)|^2}{\hbar\omega}. \quad (1)$$

( $n_c$ : excess carrier density,  $I_{Op}$ : injection current,  $\tau_c$ : carrier lifetime,  $E_{pulse}$  and  $E_{CW}$ : input light amplitudes,  $G$ : SOA gain). DISC-gate simulation method is developed using this equation, as described in Ref. 4. It has been pointed out that when  $n_c$  recovers exponentially with  $t$  between pulsed inputs as  $\exp(-t/\tau_c)$ , sub-pulses appear in the DISC output [5,6].

## 3 Comparison of measured and calculated results

Fig. 2(a) shows a typical cross-correlation trace of the 25-GHz DISC output that was measured after maximizing its extinction ratio by optimizing the MZI part. As indicated in Fig. 2(a), the extinction ratio was limited to 25 dB by small sub-pulse-like components between the output pulses. Then, for

observing the waveform of the remaining components in more details, we dropped the pulse's frequency from 25 GHz to 12.5 GHz and carefully optimized the MZI part once again. At this frequency, the extinction ratio was limited to about 18 dB by several types of relatively large sub-pulse components depending on the settings of  $Q_1$  and  $P_1$  [Figs. 2(b)-2(d)]. In particular, the sub-pulse waveform in Fig. 2(d) appeared to be time-inverted with respect to that in Fig. 2(b). After we repeatedly observed the dependences of the waveform on the waveplate angles, we estimated the relative phase bias  $\Delta\Phi_B$  from the waveplate angles by using the Jones-matrix analysis, as is indicated in each figure. ( $\Delta Q$  and  $\Delta P$  are the angles of  $Q_1$  and  $P_1$  measured from the positions where  $\Delta\Phi_B = \pi$ )

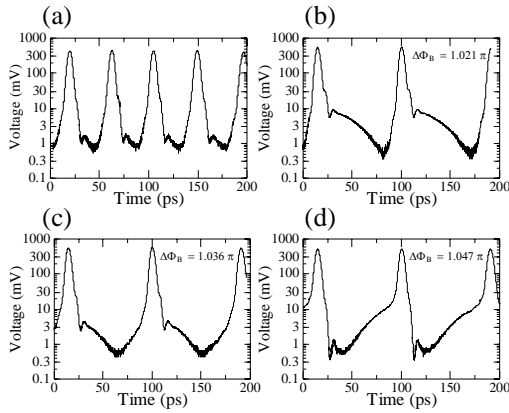


Figure 2: Cross-Correlation Traces of the DISC output signals, with different setting of  $Q_1$  and  $P_1$ . (a) with +12.3-dBm, 25-GHz input pulses, (b)-(d) with +13.5-dBm, 12.5-GHz input pulses ((b) $\Delta Q = -3^\circ$ ,  $\Delta P = -1^\circ$ , (c) $\Delta Q = -6^\circ$ ,  $\Delta P = -4^\circ$ , (d) $\Delta Q = -8^\circ$ ,  $\Delta P = -6^\circ$ )

For comparison we performed DISC simulation. Parameters on input lights were taken just same as experimental values. The SOA parameters were estimated from separate experimental results. Then sub-pulses appeared with  $-25$  dB intensity at 25 GHz (Fig. 3(a)) and with  $-20$  dB intensity at 12.5 GHz (Fig.

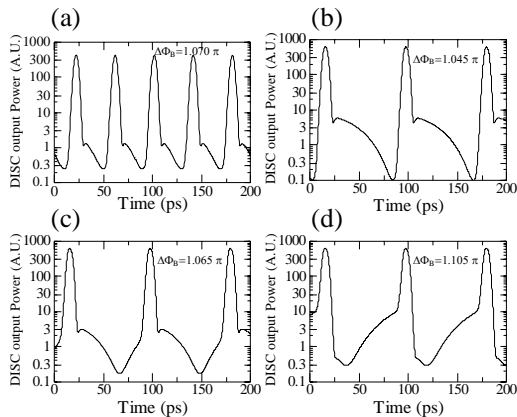


Figure 3: calculated Cross-Correlation Traces of the DISC output. (a) with 25-GHz input pulses, (b)-(d) with 12.5-GHz pulses. ((b)  $\Delta\Phi_B = 1.045\pi$ , (c)  $\Delta\Phi_B = 1.065\pi$ , (d)  $\Delta\Phi_B = 1.105\pi$ ) carrier lifetime  $\tau_c = 200$  ps, saturation energy  $P_{sat} = 1080$  fJ, Phase shift at complete carrier depletion  $\Delta\phi_{max} = +6\pi$ .

3(b)). Changes of the waveform with  $\Delta\Phi_B$  were simulated as shown in Fig 3(b)-(d).

Now the measured waveforms in Fig. 2(a)-(d) and the calculated waveforms in Fig. 3(a)-(d) match well with each other. The intensities of the sub-pulses are almost same in both cases. The changes of the waveform with the phase difference ( $\Delta\Phi_B - \pi$ ) are similar and the mismatch is only factor 2. We regard these matches as a proof of the sub-pulse generation.

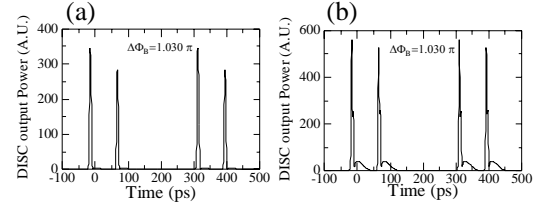


Figure 4: calculated Cross-Correlation Traces of the DISC output, showing trade-off between data-pattern independence and sub-pulse intensity. (a)  $\tau_c = 200$  ps (b)  $\tau_c = 80$  ps

The sub-pulses of the DISC may cause a serious problem when we convert patterned data signals. Fig. 4(a) shows calculated DISC output waveforms for “1100” input pulses with  $\tau_c = 200$  ps. In this case patterning effect is observed. Fig. 4(b) shows a result with smaller  $\tau_c$ . Though patterning effect could be suppressed, strong sub-pulses of  $-11$  dB also appeared. This shows that tradeoff relation exists between the sub-pulse and the pattern-induced amplitude noise.

## 4 Conclusion

We observed that the DISC output contained either small sub-pulses or sidelobes in addition to the wavelength-converted output pulses. The measured dependence of the sub-pulse waveform on the MZI setting was numerically reproduced well with our DISC model. We also showed, according to our DISC model, that a tradeoff relation exists between the magnitudes of these sub-pulses and the pattern-induced amplitude noise. These results in this work have suggested that a part of the DISC structure should be improved, for overcoming the tradeoff relation. Our on-going research activities will be presented elsewhere.

## 5 References

1. S. Nakamura et al, *Photonics Technol. Lett.* **13** (2001) 1091.
2. J. Leuthold, et al., *Electron. Lett.* **38** (2002) 890.
3. Y. Ueno et al., *Photonics Technol. Lett.* **10** (1998) 346.
4. Y. Ueno, et al., *JOSA* **B19** (2002) 2573.
5. Y. Ueno, *Jpn. J. Appl. Phys.* **43** (2004) 665.
6. M.L. Nielsen et al, *JOSA* **B21** (2004) 1606.